





Supercurrent reversal in Zeeman-split Josephson junctions

Shu-Ichiro Suzuki ¹, Yasuhiro Asano ², and Alexander A. Golubov ¹

¹Faculty of Science and Technology and MESA+ Institute for Nanotechnology, University of Twente, 7500 AE Enschede, The Netherlands

²Department of Applied Physics, Hokkaido University, Sapporo 060-8628, Japan

 (Received 17 April 2023; revised 26 September 2023; accepted 28 September 2023; published 19 October 2023)

We theoretically study the current-phase relation in a Josephson junction comprising the Zeeman-split superconductors (ZSs) and a normal metal (N). We show that at low temperatures the Josephson current in the ZS/N/ZS junctions exhibits a supercurrent reversal at a certain phase difference $\varphi_c \in (0, \pi)$. By calculating the spectral Josephson current, we demonstrate that the band splitting due to the Zeeman interaction causes the level crossing in the spectra of the Andreev bound states and the sign reversal of the Josephson current. Additionally, we propose an alternative method to observe the supercurrent reversal. Tuning the Rashba spin-orbit coupling electrically, one can control the critical phase difference φ_c , eliminating the need for manipulating two magnetizations independently.

DOI: [10.1103/PhysRevB.108.144505](https://doi.org/10.1103/PhysRevB.108.144505)

I. INTRODUCTION

A relation between the Josephson current J and the phase difference φ across a junction, called a current-phase relation (CPR), reflects various possible mechanisms of Cooper pair transport in the structure [1]. The transmission coefficients of Cooper pairs are governed by junction characteristics such as the transmission probability of the normal segment and the pairing symmetries of the superconductors. With advances in experimental techniques, CPR has recently become a measurable quantity using superconducting quantum interference devices (SQUIDs) [2–13].

The typical CPR represented as $J \propto \sin \varphi$ can be realized, for example, in a junction in which two BCS superconductors are separated by an insulator. Only the lowest-order coupling is allowed between two BCS superconductors because the transparency of an insulator is much smaller than unity. When an insulator is replaced by a highly transparent metal, higher harmonics such as $\sin(j\varphi)$ with $j > 1$ modify the CPR. With increasing the transparency to unity, the CPR at low temperatures crosses over to a sawtooth shape [14,15] with a jump at $\varphi = \pm\pi$. Recently, it has been predicted that the 4π -periodic CPR might be realized at low temperatures in a Josephson junction hosting the Majorana bound states (MBSs). The Andreev bound states (ABSs) [16,17] including the MBSs [18–22] stemming from the unconventional Cooper pairing [23–26] cause the resonant transmission of quasiparticles [27–36]. The 4π -periodic Josephson currents observed in topological superconducting junctions may indicate the realization of the MBSs [6,37,38].

At the same time, the CPR can be qualitatively modified by the Zeeman splitting (i.e., spin-splitting superconductors [39–50]). The Josephson current in the diffusive SFcFS junction has been studied using the quasiclassical Green's function method [51], where S, F, and c stand for a superconductor, a ferromagnetic metal, and a constriction, respectively. It was shown that in such structures the Josephson current at low temperatures changes the direction at an intermediate phase difference $\varphi_c \in (0, \pi)$ in addition to the standard current re-

versals at $\varphi = 0$ and π [50,51]. In other words, the CPR at a low temperature has an extra abrupt jump at the critical phase at $\varphi = \varphi_c$. Such an unusual CPR, however, has not been detected in experiments yet. To observe the current reversal at φ_c , we need to understand how to control this behavior to suggest a more feasible experimental setting.

In this paper, we study the Josephson effect between two Zeeman-splitting superconductors (ZSs) in one dimension. In particular, we investigate the mechanism of the Josephson-current reversal at φ_c and consider an experimental setup to observe this effect. Using the recursive Green's function (GF) method in the lattice model, we obtain the CPR with varying the junction parameters: magnetizations in the ZSs, junction length, and temperature. We have shown that the supercurrent reversal at φ_c takes place when the magnetizations are not antiparallel and can be the most prominent when the magnetizations are parallel at low temperatures. Analyzing a spectral Josephson current, we also show the origin of the anomalous current reversal in the CPR. We discuss the relation between the critical phase difference and the positions of Andreev levels (i.e., energy levels of the quasiparticle bound states in a junction).

In addition, we demonstrate that the shape of the CPR and the magnitude of φ_c can be controlled by varying the Rashba spin-orbit coupling (SOC) in the normal segment by an external gate, which is easier than controlling the magnetizations of the ZSs. The Rashba SOC effectively changes the magnetization configuration of the junction through the spin

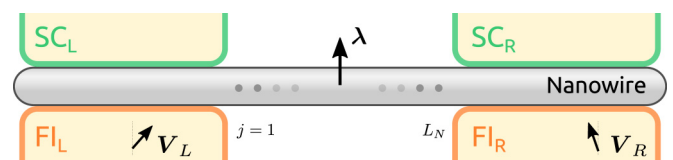


FIG. 1. Schematic of the system. The junction consists of Zeeman-split superconductors (ZSs) and a nanowire with a strong SOC. The spin-splitting directions in the SCs are characterized by $V_{L(R)}$. The length of the nanowire is characterized by L_N .

precession [52,53] in the normal segment. To control φ_c in the absence of the Rashba SOC, one has to tune the misalignment between two magnetizations in the ZSs. At the same time, by tuning the SOC strength, one can qualitatively reproduce all of the CPR types without changing the direction of the magnetizations.

II. MODEL AND FORMULATION

We consider a one-dimensional Josephson junction that consists of two ZSs. The two ZSs are separated by a normal metal with the length L_N , where we consider the Rashba SOC. The Zeeman-splitting superconducting state can be realized in the structure shown in Fig. 1, where the pair potential and the Zeeman interaction are present in the wire because of the proximity from the conventional superconductors (SCs) and the ferromagnetic insulators. The Hamiltonian in the normal segment is given by

$$\begin{aligned} \mathcal{H}_N = & -t \sum_{j,\alpha} [c_{j+1,\alpha}^\dagger c_{j,\alpha} + c_{j,\alpha}^\dagger c_{j+1,\alpha}] \\ & + i\frac{\lambda}{2} \sum_{j,\alpha,\beta} [c_{j+1,\alpha}^\dagger (\hat{\sigma}_y)_{\alpha\beta} c_{j,\beta} - c_{j,\alpha}^\dagger (\hat{\sigma}_y)_{\alpha\beta} c_{j+1,\beta}] \\ & + \sum_{j,\alpha} c_{j,\alpha}^\dagger (2t - \mu_N) c_{j,\alpha}, \end{aligned} \quad (1)$$

where t , λ , and μ_N are the hopping energy, the energy of the Rashba spin-orbit interaction, and the chemical potential in the normal metal, respectively. The creation and annihilation operators at the lattice site j with spin α are denoted by $c_{j,\alpha}^\dagger$ and $c_{j,\alpha}$, respectively. The Pauli matrices in spin and Nambu space are denoted by σ_ν and τ_ν with $\nu \in \{x, y, z\}$, respectively. The identity matrix in each space is defined as σ_0 and τ_0 . In this paper, the accents $\hat{\cdot}$ and $\check{\cdot}$ mean the 2×2 and 4×4 matrices in the spin and Nambu space, respectively. The Hamiltonian in the superconducting leads are

$$\begin{aligned} \mathcal{H}_i = & -t \sum_{j,\alpha} [c_{j+1,\alpha}^\dagger c_{j,\alpha} + c_{j,\alpha}^\dagger c_{j+1,\alpha}] \\ & + \sum_{j,\alpha} c_{j,\alpha}^\dagger [(2t - \mu_S) \hat{\sigma}_0 - \mathbf{V}_i \cdot \hat{\boldsymbol{\sigma}}]_{\alpha\beta} c_{j,\beta} \\ & + \sum_j [\Delta e^{i\varphi_i} c_{j,\uparrow}^\dagger c_{j,\downarrow}^\dagger + \text{H.c.}], \end{aligned} \quad (2)$$

with $i = L$ and R , where μ_S is the chemical potential, Δ is the amplitudes of the pair potential, and $\varphi_{L(R)}$ represents the phase of the order parameter in the left (right) SC.

The electric current is obtained from the Matsubara GF $\check{G}_{j,j'}(i\omega_n)$ in the normal segment [54–56],

$$J = \frac{ie}{2\hbar} T \sum_{\omega_n} J_n, \quad (3)$$

$$J_n = \text{Tr}\{\check{\tau}_3[\check{\tau}_+ \check{G}_{j,j+1}(i\omega_n) - \check{\tau}_- \check{G}_{j+1,j}(i\omega_n)]\}, \quad (4)$$

where $\omega_n = (2n+1)\pi T$ is the Matsubara frequency, T is the temperature, n is an integer number, and $e < 0$ is the charge of an electron. The hopping matrices are defined as

$$\check{\tau}_\pm = \begin{bmatrix} \hat{t}_\pm & 0 \\ 0 & \hat{t}_\pm^* \end{bmatrix}, \quad \hat{t}_\pm = \begin{bmatrix} -t & \mp\lambda/2 \\ \pm\lambda/2 & t \end{bmatrix}. \quad (5)$$

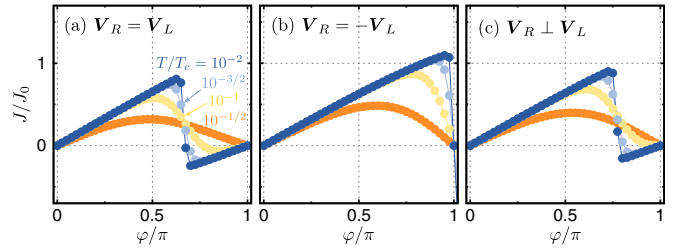


FIG. 2. Current-phase relation in a ZS/N/ZS junction *without* SOC. The amplitudes of the magnetization are set to $V = 0.5\Delta_0$. The magnetization in the left SC is $\mathbf{V}_L = V\mathbf{e}_z$ and that in the right \mathbf{V}_R is (a) $V\mathbf{e}_z$, (b) $-V\mathbf{e}_z$, and (c) $V\mathbf{e}_y$. The temperature is set to $T = T_c \times 10^{n_T}$, where n_T varies from -2 (blue line) to -0.5 (orange line) by 0.5 . The length of the junction and the chemical potential are $L_N = 80$ and $\mu_S = \mu_N = 0.5t$, respectively. The legend in (a) refers to all panels.

The Josephson current can be calculated also in the real-energy representation, which helps us to understand a relation between the Josephson current and the Andreev bound state energies. The Josephson current is represented alternatively in terms of the spectral current $J_E(E)$,

$$J = \frac{e}{2\hbar} \int J_E \tanh\left(\frac{E}{2T}\right) dE, \quad (6)$$

$$J_E = \frac{1}{2\pi} \text{Tr}\{\check{\tau}_3[\check{\tau}_+ \check{G}_{j,j+1}(E') - \check{\tau}_- \check{G}_{j+1,j}(E')]\}, \quad (7)$$

where $\check{G}_{j,j+1}(E')$ is the retarded GF with $E' = E + i\delta$ with δ being the smearing factor (i.e., an infinitesimal real number).

Throughout this paper, the Matsubara GF $\check{G}_{j,j'}(i\omega_n)$ and the retarded GF $\check{G}_{j,j'}^R(E)$ are calculated by using the recursive GF method [57]. The amplitudes of the magnetization in the ZSs are assumed to be the same ($V = V_L = V_R$ with $V_i = |V_i|$), whereas the directions of them can be different from each other. The ratio between the pair potential at $T = 0$ and the hopping energy is set to $\Delta_0 = 0.01t$. We assume that the Zeeman interaction is smaller than $0.5\Delta_0$ so that the pair potentials in the ZSs are finite [58,59]. The temperature dependence of the pair potential is calculated by the BCS relation. The current density is normalized to $J_0 = |e|\Delta_0/2\hbar$, and the smearing factor is set to $\delta = 0.02\Delta_0$. The unit of length is the lattice constant.

III. ANOMALOUS CURRENT REVERSAL IN THE JOSEPHSON CURRENT

We first show the numerical results of the CPRs *without* the SOC in Fig. 2. The amplitude of the magnetizations is set to $V = 0.5\Delta_0$. The magnetization in the left SC is fixed to $\mathbf{V}_L = V\mathbf{e}_z$. The magnetization in the right SC is (a) parallel ($\mathbf{V}_R = \mathbf{V}_L$), (b) antiparallel ($\mathbf{V}_R = -\mathbf{V}_L$), and (c) perpendicular ($\mathbf{V}_R \perp \mathbf{V}_L$) to that in the left SC. The temperature is set to $T = T_c \times 10^{n_T}$, where n_T varies from -2 (blue line) to -0.5 (orange line) by 0.5 . For the parallel configuration in Fig. 2(a), the Josephson currents at low temperatures change the direction abruptly at a certain phase difference that is neither 0 nor π . We define this phase difference as the critical phase $\varphi_c \in (0, \pi)$. Hereafter, we mainly focus on the jump in

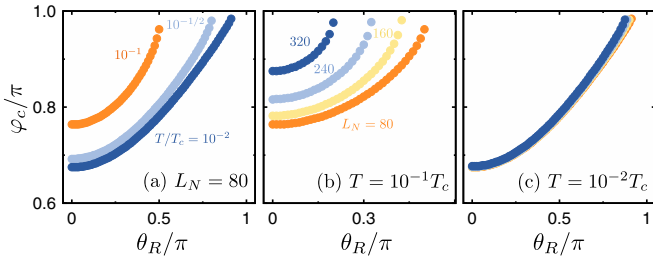


FIG. 3. (a) Temperature dependence of the critical phase in a ZS/N/ZS junction *without* SOC. The magnetization in the left is $\mathbf{V}_L = V\mathbf{e}_z$. The magnetization in the right is $\mathbf{V}_R = V(\cos\theta_R\mathbf{e}_z + \sin\theta_R\mathbf{e}_x)$. The amplitudes of the magnetization are set to $V = 0.5\Delta_0$. The temperature is set to $T = T_c \times 10^{n_T}$, where n_T varies from -2 to -1 by 0.5 . The length of the junction is $L_N = 80$. [(b),(c)] Length dependence of the critical phase. The temperature is fixed at (b) $T/T_c = 10^{-1}$ and (c) 10^{-2} . The coherence length in a normal metal is estimated as $\xi_T \approx 370$ in (b) and $\xi_T \approx 3700$ in (c). For (c), the same legend is used as in (b).

the CPR appearing at low temperatures and the dependence of φ_c on the junction parameters.

For the antiparallel configuration in Fig. 2(b), the CPR changes from the sinusoidal function at a high temperature to the sawtooth shape [14] at a low temperature. The abrupt sign change of the Josephson current occurs only at $\varphi = \pi$. The CPR at a low temperature is neither $\cos(\varphi/2)$ nor φ . This suggests that the junction at $L_N = 80$ is in the intermediate parameter region between the short junction limit $L_N \ll \xi_0$ and the long junction limit $L_N \gg \xi_0$, where $\xi_0 = \hbar v_F / 2\pi T_c$ is the coherence length and v_F is the Fermi velocity. In Fig. 2, the coherence length is estimated as $\xi_0 \approx 37$ at $\mu_S = 0.5t$. These characteristic behaviors in Figs. 2(a) and 2(b) can be also seen in the quasiclassical limit $T_c \ll \mu_S$ as shown in Appendix A. The Usadel equation can be solved analytically in the short junction limit. The analytic expression of the Josephson current helps us to understand the reasons for the presence (absence) of the current reversal in the parallel (antiparallel) configuration. For the perpendicular configuration, the abrupt sign change also appears as shown in Fig. 2(c). In this case, φ_c is larger than that in the parallel configuration in Fig. 2(a).

We show the relations between φ_c and the misalignment angle θ_R in Fig. 3, where $\mathbf{V}_L = V\mathbf{e}_z$, θ_R is defined as $\mathbf{V}_R = V(\cos\theta_R\mathbf{e}_z + \sin\theta_R\mathbf{e}_x)$ and $\mu_S = \mu_N = 0.5t$. The results in Fig. 3(a) suggest that the CPR depends sensitively on temperatures. The critical phase is calculated for several choices of the junction length L_N in Figs. 3(b) and 3(c), where we fix a temperature at $T = 0.1T_c$ in (b) and $T = 0.01T_c$ in (c). At $T = 0.1T_c$, φ_c approaches π at smaller θ_R when the junction is long.

The Josephson current can be decomposed into the harmonics as

$$J = \sum_{\ell=1}^{\infty} J_{\ell} \sin(\ell\varphi). \quad (8)$$

At a high temperature $T \lesssim T_c$, the contribution of the lowest-order term with $\ell = 1$ is dominant for any junctions because of the relation $J_{\ell} \propto \exp(-\ell L_N / \xi_T)$ [1], where $\xi_T = \hbar v_F / 2\pi T$

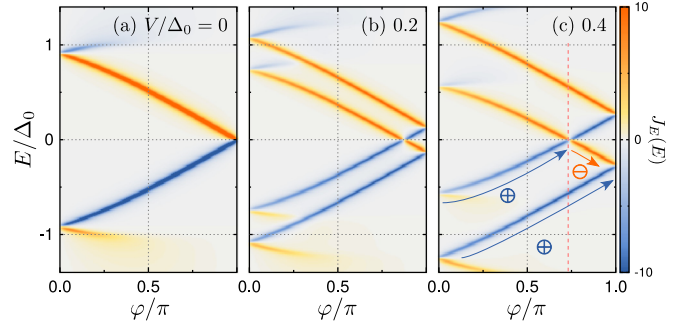


FIG. 4. Spectral Josephson currents in a ZS/N/ZS junction *without* SOC. The two magnetizations align in parallel: $\mathbf{V}_R = \mathbf{V}_L = V\mathbf{e}_z$. The amplitude of magnetization is chosen as (a) $V/\Delta_0 = 0$, (b) 0.2 , and (c) 0.4 . The junction length, the chemical potential, and the smearing factor are set to $L_N = 80$, $\mu = t$, and $\delta = 0.02\Delta_0$, respectively. The signs in (c) indicate the sign of the contribution to the total current.

is the coherence length at a clean metal. In this temperature regime, the CPR is always sinusoidal. To obtain the current reversal at φ_c , the CPR needs to deviate from the standard sinusoidal function. At a very low temperature $T \ll T_c$, the contributions of the higher harmonics can modify the CPR, leading to the abrupt sign change of the Josephson current. At $T = 0.1T_c$ [Fig. 3(b)], the amplitudes of higher harmonics rapidly decrease with increasing L_N . Thus, φ_c at $\theta_R = 0$ increases to π with increasing L_N in Fig. 3(b).

At a higher temperature [Fig. 3(b)], the abrupt sign change occurs only when L_N is sufficiently short. In a long junction (i.e., $L_N > \xi_T$), the higher harmonics are sufficiently large to change the CPR from the standard sinusoidal shape. At a sufficiently low temperature $T = 0.01T_c$ [Fig. 3(c)], on the other hand, φ_c is independent of L_N because the contributions of the higher harmonics to the Josephson current are sufficiently large even when $L_N = 320$. In Figs. 3(b) and 3(c), the thermal coherence lengths are estimated as $\xi_T \approx 370$ and $\xi_T \approx 3700$, respectively.

Figure 3 also shows that φ_c is minimum at $\theta_R = 0$ and approaches π with increasing θ_R . The abrupt sign reversal does not occur when the misalignment angle is large. In particular, in a long junction [Fig. 3(b)], the current reversal occurs only when the misalignment angle is smaller than a certain value, the maximum misalignment angle. As L_N increases, the maximum misalignment angle decreases. Currently, there is no intuitive picture that explains this behavior.

The origin of the current reversal at φ_c can be understood by the level splitting in the Andreev bound state energy due to Zeeman fields. The spectral Josephson currents $J_E(E)$ in Eq. (7) are shown in Fig. 4, where we fix (a) $V/\Delta_0 = 0$, (b) 0.2 , and (c) 0.4 with $\mathbf{V}_L = \mathbf{V}_R$, and $L_N = 80$. The relation between J_E and J is presented in Eq. (6). In the absence of the magnetization, the spectral Josephson current has peaks around $E = \pm\Delta_0(1 - \varphi/\pi)$ as shown in Fig. 4(a). Since the junction at $L_N = 80$ is not in the long-junction limit, the calculated results in Fig. 4(a) deviate slightly from such a linear relation. The spectra are doubly degenerate due to spin degree of freedom at $V = 0$. For finite V , Zeeman fields lift the degeneracy by $\pm V$ as shown in Figs. 4(b) and 4(c). At $E = 0$,

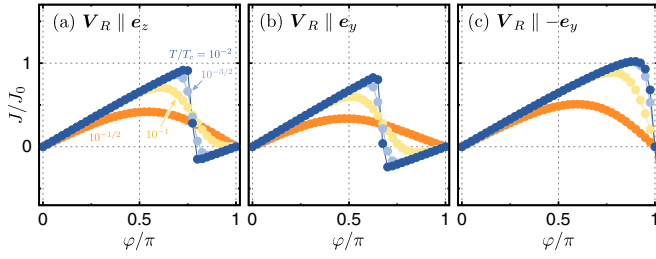


FIG. 5. Current-phase relation in a ZS/NW/ZS junction with the SOC. The amplitude of the SOC in the NW is set to $\lambda = 0.5t$. The magnetization in the left superconductor is $\mathbf{V}_L = V\mathbf{e}_y$. The magnetization in the right superconductor is (a) $\mathbf{V}_R = V\mathbf{e}_y$, (b) $\mathbf{V}_R = -V\mathbf{e}_y$, and (c) $\mathbf{V}_R = V\mathbf{e}_z$. The other parameters are set to the same values as those used in Fig. 2. The legend in (a) refers to all panels.

the two branches cross at $\varphi = \varphi_c$. Near $E = 0$, the branch for $\varphi < \varphi_c$ and that for $\varphi > \varphi_c$ contribute to the Josephson current in the opposite way as indicated by the signs in Fig. 4(c). This explains the abrupt change in the Josephson current at $\varphi = \varphi_c$. In Appendix A, we show that the CPR for the short junction limit indicates qualitatively the same behavior by solving the quasiclassical Usadel equation.

In the quasiclassical limit ($T_c \ll \mu$), the contributions from the two branches to the Josephson current cancel perfectly and the total current becomes zero (see Appendix A for details). However, in finite-length Josephson junctions, the total current is still finite at $\varphi_c < \varphi < \pi$ as shown in Figs. 2(a) and 2(c). This would be because of, for example, the thermal decoherence or extra bound states trapped in the normal segment.

IV. CONTROLLING THE CRITICAL PHASE DIFFERENCE

The current-phase relation *with* the SOC are shown in Fig. 5, where we set $\lambda = 0.5t$ and $\mathbf{V}_L = V\mathbf{e}_y$. The magnetization in the right SC is (a) $\mathbf{V}_R = V\mathbf{e}_y$, (b) $\mathbf{V}_R = -V\mathbf{e}_y$, and (c) $\mathbf{V}_R = V\mathbf{e}_z$. The CPRs shown in Fig. 5 are qualitatively the same as those in Fig. 2. Namely, the SOC does not affect the CPR in these magnetic configurations. The Hamiltonian of the SOC represented as

$$\mathcal{H}_{\text{SOC}} = \lambda \sin(k) \hat{\sigma}_y, \quad (9)$$

in momentum space. The CPR is insensitive to the SOC in a junction in which one of the Zeeman fields points the \mathbf{e}_y direction. We have also confirmed that φ_c is also insensitive to λ for $\mathbf{V}_L = V\mathbf{e}_y$ (not shown). The sensitivity of the CPR to the SOC depends on the magnetic configurations of the junction as discussed below.

When the magnetic moments in the two superconductors are perpendicular to \mathbf{e}_y , the CPR shows a qualitatively different behavior from those in Fig. 5. The direction of a Zeeman field in the left SC is fixed at $\mathbf{V}_L = V\mathbf{e}_z$. The CPRs for the parallel configuration with $\mathbf{V}_R = V\mathbf{e}_z$ are shown in Figs. 6(a)–6(e) where $V = 0.5\Delta_0$, $L_N = 80$, $\mu_S = \mu_N = t$, and the amplitude of the SOC varies from (a) $\lambda = 0.5t$ to (e) $0.1t$ by $-0.1t$. The critical phase φ_c changes depending on the amplitudes of the SOC. We also show the results for the perpendicular configuration with $\mathbf{V}_R = V\mathbf{e}_x$ in Figs. 6(f)–6(j). The dependence of φ_c on λ in the perpendicular configuration

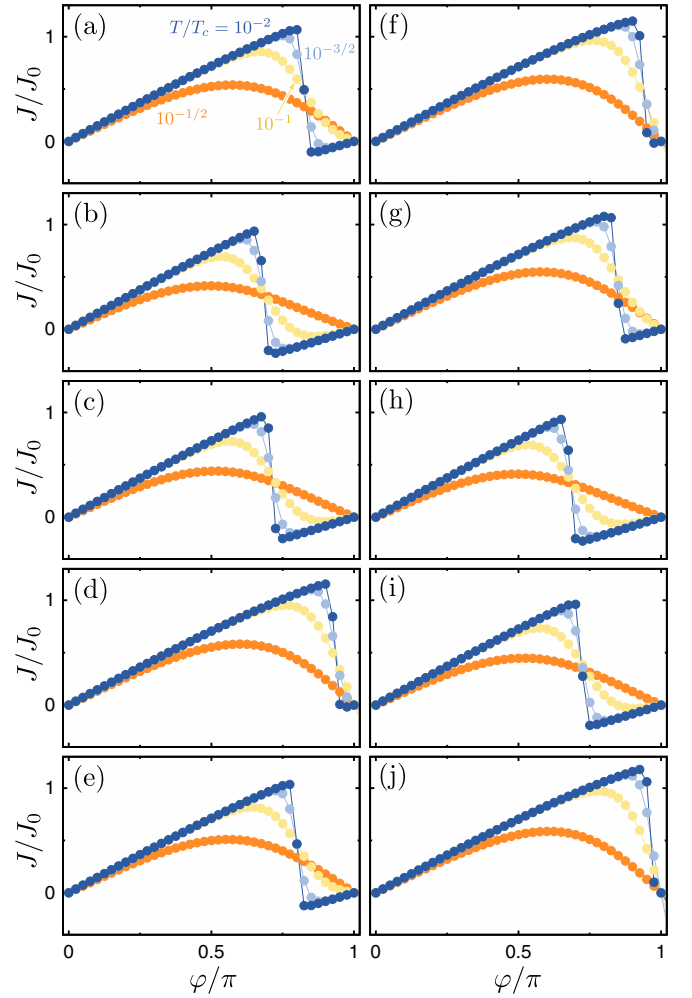


FIG. 6. Current-phase relation of ZS/NW/ZS junctions with the SOC. The Zeeman field in the left SC is $\mathbf{V}_L = V\mathbf{e}_z$. The Zeeman field in the right SC $\mathbf{V}_R = V\mathbf{e}_z$ is parallel to \mathbf{V}_L in [(a)–(e)]. The strength of the SOC varies from (a) $\lambda = 0.5t$ to (e) $0.1t$ by $-0.1t$. The Zeeman field in the right SC $\mathbf{V}_R = V\mathbf{e}_x$ is perpendicular to \mathbf{V}_L in [(f)–(j)]. These results are plotted in the same manner as in [(a)–(e)]. The junction length and the chemical potential are fixed at $L_N = 80$ and $\mu_S = \mu_N = t$, respectively. The legend in (a) refers to all panels.

in Figs. 6(f)–6(j) is different from that in the parallel configuration in Figs. 6(a)–6(e). The calculated results show that φ_c can be controlled by the amplitude of the SOC.

In Fig. 7, φ_c is plotted as a function of the junction length L_N for several choices of λ , where $\mathbf{V}_L = \mathbf{V}_R = V\mathbf{e}_z$, $V = 0.5\Delta_0$, and a temperature is fixed at $T = 0.01T_c$. The results show that φ_c oscillates as a function of L_N . The abrupt sign change in the Josephson current disappears for several specific lengths L_N at which φ_c becomes π . From the numerical results, we find that the period of the oscillation is approximately proportional to λ^{-1} . The oscillating behavior originates from the spin precession due to the SOC as discussed in Refs. [49,52,53]. The quasiparticles have an additional phase shift depending on their spin while they travel across the normal wire.

The SOC also affects the spectral current as shown in Fig. 8, where $\mathbf{V}_L = \mathbf{V}_R = V\mathbf{e}_z$ with $V = 0.5t$, $L_N = 80$ and

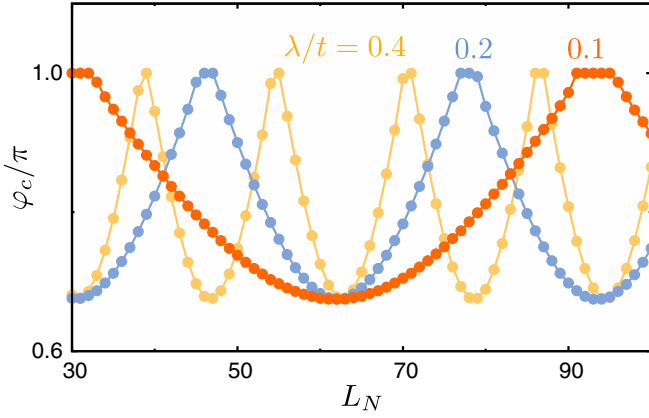


FIG. 7. The critical phase φ_c is plotted as a function of the length of normal segment L_N for several choices of λ . The magnetizations are set to $\mathbf{V}_L = \mathbf{V}_R = V\mathbf{e}_z$ with $V = 0.5\Delta_0$ and the temperature is fixed at $T = 0.01T_c$.

the SOC varies from $\lambda/t = 0.4$ to 0.6 by 0.1 . At $\lambda/t = 0.4$, the amplitude of the band splitting δE is almost maximum. As a consequence, φ_c takes its minimum as shown in Fig. 7. With increasing λ , δE decreases and almost vanishes at $\lambda/t = 0.6$. As a consequence, the anomalous current reversal does not occur at $\lambda/t = 0.6$. The numerical results show that δE changes periodically as a function of λ . The result in Figs. 8(a) [8(c)] corresponds to one of the maxima (minima) of δE . The magnitude of the band splitting in the spectral current is consistent with those obtained in the continuum model [49]. In the continuous limit, the band splitting is estimated as $\delta E = V \cos(\lambda L_N / \hbar v_F)$. From this relation with $\mu_N = t$, the period of the oscillation in Fig. 7 is estimated as $L_0 \sim 5.44t/\lambda$, which is almost consistent with our numerical simulation.

In the original paper by one of the authors, there is no controlling parameter in a SFcFS junction after fabrication. Thus the current reversal can be detected only by tuning the phase difference φ . The results in Fig. 6 suggest that the current reversal occurs at a fixed phase φ by changing the amplitude of SOC in the normal segment λ . Observing the current reversal would be easier in the Josephson junction proposed in this paper because fine-tuning λ is possible by adjusting the gate voltage.

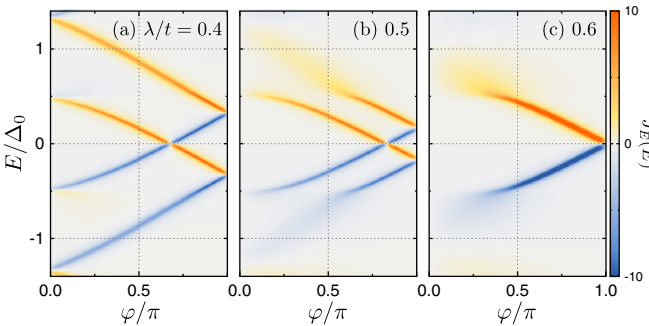


FIG. 8. Spectral currents in the parallel configuration are plotted for several choices of the amplitude of SOC as (a) $\lambda = 0.4t$, (b) $0.5t$, and (c) $0.6t$. The other parameters are set to the same values as those in Figs. [6(a)–6(e)].

V. CONCLUSIONS

We have studied an unusual current-phase ($J - \varphi$) relation (CPR) of a Josephson junction that consists of two Zeeman-splitting superconductors (ZSs). At a low temperature, the Josephson current changes its direction abruptly at a critical phase difference $\varphi_c \in (0, \pi)$. The results show that φ_c depends sensitively on the arrangement between the two magnetizations in the two ZSs. The most pronounced current jumps are observed in the parallel configuration, while no current jumps are seen in the antiparallel configuration. Analyzing the spectral Josephson current, we have shown that the current reversal is due to the energy splitting of the Andreev bound state by the Zeeman potential. In the parallel configuration, the Josephson current changes direction at $\varphi = \varphi_c$ because a pair of the Andreev levels cross at zero energy. In the antiparallel configuration, however, the current reversal disappears. This is because the two magnetizations in opposite directions cancel each other's effect on the Andreev levels. The current reversal also occurs when the two magnetizations are perpendicular to each other. Namely, the cancellation is absent in the perpendicular magnetic configuration.

In addition, we have demonstrated that φ_c depends on the Rashba spin-orbit interaction introduced in the normal segment. The spin precession of a quasiparticle due to the spin-orbit interaction modifies the energy spectra of the Andreev levels and φ_c . In experiments, the amplitude of the spin-orbit interaction is tunable by applying the gate voltage. Therefore, by measuring the CPR by tuning the spin-orbit coupling, one would be able to observe the anomalous current reversal.

ACKNOWLEDGMENTS

The authors are grateful to Ya. V. Fominov and C. Li for the useful discussions. S.-I.S. acknowledges Overseas Research Fellowships by JSPS and the hospitality at the University of Twente.

APPENDIX A: QUASICLASSICAL GREEN'S FUNCTION THEORY

1. Usadel equation

In a superconducting proximity structure in the quasiclassical limit $\mu_S \gg T_c$, the solution of the Usadel equation

$$\hbar D \nabla \cdot (\check{g} \nabla \check{g}) + i[i\omega_n \check{\tau}_3 + \check{H}, \check{g}]_- = 0, \quad (\text{A1})$$

describes well superconducting phenomena, where D is the diffusion constant and $\check{g} = \check{g}(\mathbf{r}, i\omega_n)$ is the Matsubara Green's function in the Nambu space (i.e., particle-hole \otimes spin space) defined as

$$\check{g} = \begin{pmatrix} \hat{g} & \hat{f}_\omega \\ \hat{f}_{-\omega}^\dagger & -\hat{g} \end{pmatrix}. \quad (\text{A2})$$

In Eq. (A2), we have used the symmetry relation between the anomalous Green's function, $-\hat{f}_\omega = \hat{f}_{-\omega}^\dagger$, where the under-tilde functions are defined by $\tilde{X}(\mathbf{r}, i\omega_n) = \tilde{X}(\mathbf{r}, i\omega_n)^*$ with X being an arbitral function. In the presence of a Zeeman field

$V = V\mathbf{e}_z$, the \check{H} matrix is given by

$$\check{H} = \begin{bmatrix} \hat{\xi} & \hat{\eta} \\ \hat{\eta} & \hat{\xi} \end{bmatrix} = \begin{bmatrix} -V\hat{\sigma}_z & i\Delta_0(i\hat{\sigma}_y) \\ i\Delta_0^*(i\hat{\sigma}_y)^\dagger & -V\hat{\sigma}_z \end{bmatrix}, \quad (\text{A3})$$

where we have assumed the Zeeman potential $V(x)$ depends on the spatial coordinate x . In this case, it is convenient to apply the unitary transform,

$$\check{U}^{-1}(i\omega_n\check{\tau}_3 + \check{H})\check{U} \quad (\text{A4})$$

$$= \begin{bmatrix} i\omega_n - V\hat{\sigma}_z & i\Delta_0\hat{\sigma}_0 \\ i\Delta_0^*\hat{\sigma}_0 & -i\omega_n + V\hat{\sigma}_z \end{bmatrix}, \quad (\text{A5})$$

with $\check{U} = \text{diag}[\hat{\sigma}_0, -i\hat{\sigma}_y]$. Accordingly, the Green's function can be parametrized as

$$\check{U}^{-1}\check{g}\check{U} = \begin{pmatrix} g_+ & 0 & f_{\omega,+} & 0 \\ 0 & g_- & 0 & f_{\omega,-} \\ f_{-\omega,+}^* & 0 & -g_- & 0 \\ 0 & f_{-\omega,-}^* & 0 & -g_+ \end{pmatrix}, \quad (\text{A6})$$

where we have used $\hat{g} = \text{diag}[g_+, g_-]$ and $\hat{f}_\omega = \text{diag}[f_{\omega,+}, f_{\omega,-}](i\hat{\sigma}_y)$. The Usadel equation in 4×4 space can be reduced into two Usadel equations in 2×2 space. The Green's function in each spin subspace can be described as

$$\tilde{g}_\sigma = \begin{pmatrix} g_{\omega,\sigma} & f_{\omega,\sigma} \\ f_{-\omega,\sigma}^* & -g_{\omega,\bar{\sigma}} \end{pmatrix} = \begin{pmatrix} g_{\omega,\sigma} & f_{\omega,\sigma} \\ \underline{f}_{-\omega,\sigma} & -g_{\omega,\bar{\sigma}} \end{pmatrix}, \quad (\text{A7})$$

where $\sigma = \pm$ (with $\bar{\sigma} = -\sigma$) specifies the spin subspace. We have introduced the underline accent as $\underline{f}_\omega = f_{-\omega}^*$. The normalization condition becomes

$$g^2 + f\underline{f} = 1. \quad (\text{A8})$$

In the homogeneous limit, the Green's functions satisfy

$$\tilde{g}_\sigma = \frac{1}{\Omega_\sigma} \begin{bmatrix} \omega_\sigma & \Delta_0 \\ \Delta_0^* & -\omega_\sigma \end{bmatrix}, \quad (\text{A9})$$

with $\Omega_\sigma = \sqrt{\omega_\sigma^2 + |\Delta_0|^2}$ and $\omega_\sigma = \omega_n + i\sigma V$.

2. Josephson current

We consider a superconductor/constriction/superconductor (ScS) junction as discussed, for example, in Ref. [51]. The Josephson current in an ScS junction can be written as

$$J = \frac{\pi T}{i|e|R_N} \sum_{\omega_n, \sigma} J_\sigma(i\omega_n), \quad (\text{A10})$$

$$J_\sigma = \frac{(f_{L,\sigma} f_{R,\sigma} - f_{L,\sigma} \underline{f}_{R,\sigma})/2}{2 - D[1 - g_{L,\sigma} g_{R,\sigma} - (f_{L,\sigma} f_{R,\sigma} + f_{L,\sigma} \underline{f}_{R,\sigma})/2]}, \quad (\text{A11})$$

where the subscript $i = L$ (R) specifies the left (right) superconductor [60]. In two Zeeman-splitting superconductors, the Green's functions are given by

$$g_{i,\sigma} = \omega_{i,\sigma}/\Omega_{i,\sigma}, \quad f_{i,\sigma} = \Delta_0 e^{i\varphi_i}/\Omega_{i,\sigma}, \quad (\text{A12})$$

where $\omega_{i,\sigma} = \omega_n + i\sigma V_i$, $\Omega_{i,\sigma} = \sqrt{\omega_{i,\sigma}^2 - \Delta_0^2}$. The current across the junction can be obtained as

$$I = \frac{\pi T}{i|e|R_N} \sum_{\omega_n, \sigma} J_\sigma(i\omega_n), \quad (\text{A13})$$

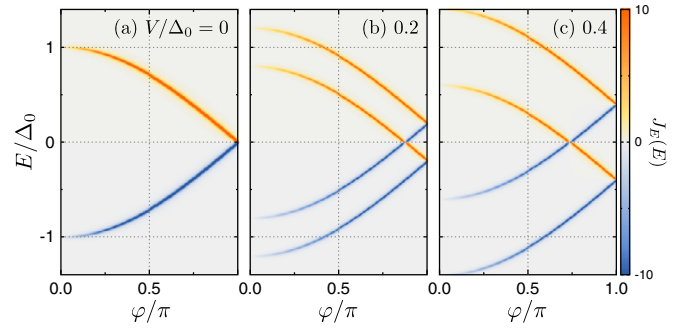


FIG. 9. Spectral Josephson current in ScS junction obtained by solving the Usadel equation.

$$J_\sigma(i\omega_n) = \frac{i\Delta_0^2 \sin \varphi}{Z_\sigma}, \quad (\text{A14})$$

$$Z_\sigma = 2\Omega_{L,\sigma}\Omega_{R,\sigma} - D[\Omega_{L,\sigma}\Omega_{R,\sigma} - \omega_{L,\sigma}\omega_{R,\sigma} - \Delta_0^2 \cos \varphi]. \quad (\text{A15})$$

When the magnetizations are parallel ($\mathbf{V}_L = \mathbf{V}_R$), the current density is reduced to

$$I = \frac{2\pi T}{|e|R_N} \sum_{\omega_n > 0} \frac{A\Delta_0^2 \sin \varphi}{A^2 + 4\omega_n^2 V^2}, \quad (\text{A16})$$

$$A = (\omega_n^2 - V^2) + \Delta_0^2[1 - D \sin^2(\varphi/2)]. \quad (\text{A17})$$

In this expression, the factor A changes the sign at

$$\sin^2(\varphi_c/2) = \frac{\Delta_0^2 - V^2 + \omega_n^2}{D\Delta_0^2}. \quad (\text{A18})$$

The results indicate that the Josephson current suddenly changes direction at a certain phase difference φ_c (i.e., anomalous current reversal in the Josephson current). In the antiparallel junction ($\mathbf{V}_L = -\mathbf{V}_R$), such an additional jump is absent in CPR. The extra phases derived from the two Zeeman fields cancel each other because of $\omega_R = \omega_L^*$ and $\Omega_R = \Omega_L^*$.

Applying the analytic continuation, the expression of the current in the real-energy representation can be obtained. In

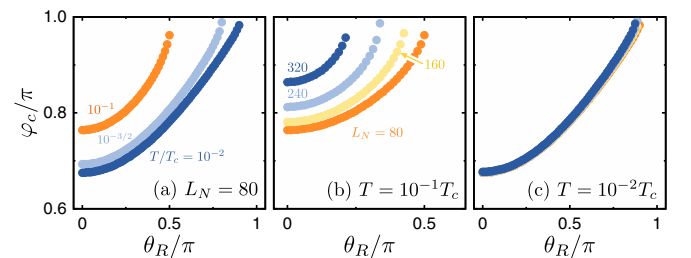


FIG. 10. (a) Temperature dependence of critical phase in ZS/NW/ZS junction. [(b),(c)] Length dependence of critical phase. The magnetization in the left is $\mathbf{V}_L = V\mathbf{e}_y$. The magnetization in the right is $\mathbf{V}_R = V(\cos \theta_R \mathbf{e}_y + \sin \theta_R \mathbf{e}_z)$. The results are shown in the same manner as in Fig. 3.

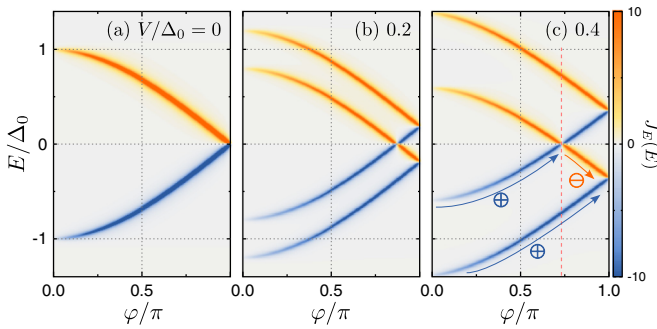


FIG. 11. Spectral Josephson currents in ZS/N/ZS junction without SOC. The parameters are set to the same values as used in Fig. 4. However, the junction length is set to $L_N = 20$.

the parallel configuration, the current in terms of the spectral current is given by

$$J = \frac{\pi}{2|e|R_N} \int J_E \tanh\left(\frac{E}{2T}\right) dE, \quad (\text{A19})$$

$$J_E = -\frac{1}{2\pi}(J^R - J^A), \quad (\text{A20})$$

$$J^R = \sum_{\sigma} \frac{i\Delta_0^2 \sin \varphi}{\Delta_0^2 [1 - D \sin^2(\varphi/2)] - (\bar{E} - \sigma V)^2}. \quad (\text{A21})$$

where $\bar{E} = E + i\delta$. Using the relation $J^A = -(J^R)^*$, we have

$$J_E = \sum_{\sigma} J_{E,\sigma}, \quad (\text{A22})$$

$$J_{E,\sigma} = \frac{1}{2\pi} \frac{\delta_1}{\Delta_1^2 + \delta_1^2} \text{sgn}[E - \sigma V] \Delta_0^2 \sin \varphi, \quad (\text{A23})$$

$$\Delta_1 = \Delta_0^2 [1 - D \sin^2(\varphi/2)] - (E - \sigma V)^2, \quad (\text{A24})$$

with $\delta_1 = 2|E - \sigma V|\delta$. Equation (A23) becomes the Lorentzian-type Dirac function at $\delta_1 \rightarrow 0$ that has peaks at

$$E = \pm \sqrt{1 - D \sin^2(\varphi/2)} + \sigma V. \quad (\text{A25})$$

The spectra reproduce the results in the high-transparency limit in both the absence and the presence of a Zeeman field [49,61]. The peak positions are shifted by a Zeeman field in a superconductor. The spectral currents J_E are shown in Fig. 9, where (a) $V/\Delta_0 = 0$, (b) 0.2, and (c) 0.4. The results are qualitatively the same as those in Fig. 4.

APPENDIX B: CRITICAL PHASE DIFFERENCE WITH SPIN-ORBIT COUPLING

In this Appendix, we discuss φ_c in the presence of the Rashba SOC. Note that one of the Zeeman interactions has the same matrix structure as that of the Rashba SOC (i.e., $V_i \cdot \hat{\sigma} \sim V_i \hat{\sigma}_2 \sim k \hat{\sigma}_2$). The results are shown in Fig. 10 in the same manner as in Fig. 3, where the results without the SOC are shown. Figure 10 shows that, when the one of the Zeeman interactions is proportional to $\hat{\sigma}_y$, the SOC with $k_x \hat{\sigma}_y$ does not qualitatively change φ_c .

APPENDIX C: SPECTRAL JOSEPHSON CURRENT IN SHORT JUNCTIONS

In this Appendix, we discuss the spectral Josephson junction without the SOC. The results are shown in Fig. 11, where the junction length is shorter ($L_N = 20$) than that in Fig. 4 ($L_N = 80$). When the junction length is sufficiently short, the Andreev level obeys $E = \pm \Delta_0 \cos(\varphi/2)$, which is analytically obtained by the Usadel theory. Moreover, the additional branches do not appear.

- [1] A. A. Golubov, M. Yu. Kupriyanov, and E. Il'ichev, *Rev. Mod. Phys.* **76**, 411 (2004).
- [2] M. L. Della Rocca, M. Chauvin, B. Huard, H. Pothier, D. Esteve, and C. Urbina, *Phys. Rev. Lett.* **99**, 127005 (2007).
- [3] G.-H. Lee, S. Kim, S.-H. Jhi, and H.-J. Lee, *Nat. Commun.* **6**, 6181 (2015).
- [4] G. Nanda, J. L. Aguilera-Servin, P. Rakyta, A. Kormányos, R. Kleiner, D. Koelle, K. Watanabe, T. Taniguchi, L. M. K. Vandersypen, and S. Goswami, *Nano Lett.* **17**, 3396 (2017).
- [5] A. Murani, A. Kasumov, S. Sengupta, Yu. A. Kasumov, V. T. Volkov, I. I. Khodos, F. Brisset, R. Delagrangé, A. Chepelianskii, R. Deblock *et al.*, *Nat. Commun.* **8**, 15941 (2017).
- [6] C. Li, J. C. de Boer, B. de Ronde, S. V. Ramankutty, E. van Heumen, Y. Huang, A. de Visser, A. A. Golubov, M. S. Golden, and A. Brinkman, *Nat. Mater.* **17**, 875 (2018).
- [7] L. V. Ginzburg, I. E. Batov, V. V. Bol'ginov, S. V. Egorov, V. I. Chichkov, A. E. Shchegolev, N. V. Klenov, I. I. Soloviev, S. V. Bakurskiy, and M. Yu. Kupriyanov, *JETP Lett.* **107**, 48 (2018).
- [8] M. Kayyalha, M. Kargarian, A. Kazakov, I. Miotkowski, V. M. Galitski, V. M. Yakovenko, L. P. Rokhinson, and Y. P. Chen, *Phys. Rev. Lett.* **122**, 047003 (2019).
- [9] F. Nichele, E. Portolés, A. Fornieri, A. M. Whicar, A. C. C. Drachmann, S. Gronin, T. Wang, G. C. Gardner, C. Thomas, A. T. Hatke, M. J. Manfra, and C. M. Marcus, *Phys. Rev. Lett.* **124**, 226801 (2020).
- [10] M. Kayyalha, A. Kazakov, I. Miotkowski, S. Khlebnikov, L. P. Rokhinson, and Y. P. Chen, *npj Quantum Mater.* **5**, 7 (2020).
- [11] Ya. V. Fominov and D. S. Mikhailov, *Phys. Rev. B* **106**, 134514 (2022).
- [12] M. Endres, A. Kononov, H. S. Arachchige, J. Yan, D. Mandrus, K. Watanabe, T. Taniguchi, and C. Schönenberger, *Nano Lett.* **23**, 4654 (2023).
- [13] I. Babich, A. Kudriashov, D. Baranov, and V. Stolyarov, *Nano Lett.* **23**, 6713 (2023).
- [14] I. O. Kulik and A. N. Omel'yanchuk, *Zh. Eksp. Teor. Fiz.* **21**, 216 (1975) [*JETP Lett.* **21**, 96 (1975)].
- [15] C. Ishii, *Prog. Theor. Phys.* **44**, 1525 (1970); **47**, 1464 (1972).
- [16] J. Hara and K. Nagai, *Prog. Theor. Phys.* **76**, 1237 (1986).
- [17] C.-R. Hu, *Phys. Rev. Lett.* **72**, 1526 (1994).
- [18] M. Sato, Y. Takahashi, and S. Fujimoto, *Phys. Rev. Lett.* **103**, 020401 (2009).
- [19] R. M. Lutchyn, J. D. Sau, and S. Das Sarma, *Phys. Rev. Lett.* **105**, 077001 (2010).
- [20] Y. Oreg, G. Refael, and F. von Oppen, *Phys. Rev. Lett.* **105**, 177002 (2010).
- [21] R. S. Akzyanov, A. L. Rakhmanov, A. V. Rozhkov, and F. Nori, *Phys. Rev. B* **94**, 125428 (2016).

- [22] S.-I. Suzuki, Y. Kawaguchi, and Y. Tanaka, *Phys. Rev. B* **97**, 144516 (2018).
- [23] S.-I. Suzuki and Y. Asano, *Phys. Rev. B* **89**, 184508 (2014); S.-I. Suzuki, *ibid.* **91**, 214510 (2015); **94**, 155302 (2016).
- [24] S.-I. Suzuki, T. Hirai, M. Eschrig, and Y. Tanaka, *Phys. Rev. Res.* **3**, 043148 (2021).
- [25] S.-I. Suzuki, S. Ikegaya, and A. A. Golubov, *Phys. Rev. Res.* **4**, L042020 (2022).
- [26] S. Yoshida, S.-I. Suzuki, and Y. Tanaka, *Phys. Rev. Res.* **4**, 043122 (2022).
- [27] Y. Tanaka and S. Kashiwaya, *Phys. Rev. Lett.* **74**, 3451 (1995).
- [28] S. Kashiwaya and Y. Tanaka, *Rep. Prog. Phys.* **63**, 1641 (2000).
- [29] Y. Asano, Y. Tanaka, and S. Kashiwaya, *Phys. Rev. B* **69**, 134501 (2004).
- [30] D. Daghero, M. Tortello, G. A. Ummarino, J.-C. Griveau, E. Colineau, R. Eloirdi, A. B. Shick, J. Kolorenc, A. I. Lichtenstein, and R. Caciuffo, *Nat. Commun.* **3**, 786 (2012).
- [31] S. Ikegaya, S.-I. Suzuki, Y. Tanaka, and Y. Asano, *Phys. Rev. B* **94**, 054512 (2016).
- [32] L. Aggarwal, A. Gaurav, G. Thakur, Z. Haque, A. K. Ganguli, and G. Sheet, *Nat. Mater.* **15**, 32 (2016).
- [33] L. A. B. Olde Olthof, S.-I. Suzuki, A. A. Golubov, M. Kunieda, S. Yonezawa, Y. Maeno, and Y. Tanaka, *Phys. Rev. B* **98**, 014508 (2018).
- [34] S.-I. Suzuki, M. Sato, and Y. Tanaka, *Phys. Rev. B* **101**, 054505 (2020).
- [35] Y. Takabatake, S.-I. Suzuki, and Y. Tanaka, *Phys. Rev. B* **103**, 184515 (2021).
- [36] S. Ikegaya, S.-I. Suzuki, Y. Tanaka, and D. Manske, *Phys. Rev. Res.* **3**, L032062 (2021).
- [37] J. Wiedenmann, E. Bocquillon, R. S. Deacon, S. Hartinger, O. Herrmann, T. M. Klapwijk, L. Maier, C. Ames, C. Brüne, C. Gould *et al.*, *Nat. Commun.* **7**, 10303 (2016).
- [38] A.-Q. Wang, C.-Z. Li, C. Li, Z.-M. Liao, A. Brinkman, and D.-P. Yu, *Phys. Rev. Lett.* **121**, 237701 (2018).
- [39] R. Meservey, P. M. Tedrow, and P. Fulde, *Phys. Rev. Lett.* **25**, 1270 (1970).
- [40] R. Meservey and P. Tedrow, *Phys. Rep.* **238**, 173 (1994).
- [41] F. S. Bergeret, A. F. Volkov, and K. B. Efetov, *Phys. Rev. Lett.* **86**, 3140 (2001).
- [42] X. Li, Z. Zheng, D. Y. Xing, G. Sun, and Z. Dong, *Phys. Rev. B* **65**, 134507 (2002).
- [43] Y. Asano, Y. Sawa, Y. Tanaka, and A. A. Golubov, *Phys. Rev. B* **76**, 224525 (2007).
- [44] F. Giazotto and F. Taddei, *Phys. Rev. B* **77**, 132501 (2008).
- [45] T. Yokoyama, M. Eto, and Y. V. Nazarov, *Phys. Rev. B* **89**, 195407 (2014).
- [46] H. Emamipour, *Chin. Phys. B* **23**, 057402 (2014).
- [47] M. Eschrig, *Rep. Prog. Phys.* **78**, 104501 (2015).
- [48] J. Linder and J. W. A. Robinson, *Nat. Phys.* **11**, 307 (2015).
- [49] T. Hashimoto, A. A. Golubov, Y. Tanaka, and J. Linder, *Phys. Rev. B* **96**, 134508 (2017).
- [50] A. Maiani, K. Flensberg, M. Leijnse, C. Schrade, S. Vaitieknas, and R. S. Souto, *Phys. Rev. B* **107**, 245415 (2023).
- [51] A. A. Golubov, M. Yu. Kupriyanov, and Ya. V. Fominov, *JETP Lett.* **75**, 588 (2002).
- [52] S. Datta and B. Das, *Appl. Phys. Lett.* **56**, 665 (1990).
- [53] A. Manchon, H. C. Koo, J. Nitta, S. M. Frolov, and R. A. Duine, *Nat. Mater.* **14**, 871 (2015).
- [54] A. Furusaki, *Physica B (Amsterdam)* **203**, 214 (1994).
- [55] Y. Asano, *Phys. Rev. B* **63**, 052512 (2001).
- [56] Y. Asano, *Phys. Rev. B* **64**, 224515 (2001).
- [57] P. A. Lee and D. S. Fisher, *Phys. Rev. Lett.* **47**, 882 (1981).
- [58] A. M. Clogston, *Phys. Rev. Lett.* **9**, 266 (1962).
- [59] B. S. Chandrasekhar, *Appl. Phys. Lett.* **1**, 7 (1962).
- [60] A. V. Zaitsev, *Zh. Eksp. Teor. Fiz.* **86**, 1742 (1984) [*JETP* **59**, 1015 (1984)].
- [61] I. O. Kulik, *Zh. Eksp. Teor. Fiz.* **49**, 1211 (1966) [*JETP* **22**, 841 (1966)].